DISTRIBUTION STATEMENT A. Approved for public release: distribution is unlimited. 88ABW Cleared 02/28/017; 88ABW-2017-0800.

Measurements of pulse rate using long-range imaging photoplethysmography and sunlight illumination outdoors

Ethan B. Blackford*[a], Justin R. Estepp*[b]
[a]Ball Aerospace, 2875 Presidential Drive, Fairborn, OH USA 45324-6269;
[b]711th Human Performance Wing, US Air Force Research Laboratory, 2510 Fifth Street, Wright-Patterson AFB, OH USA 45433-7951

ABSTRACT

Imaging photoplethysmography, a method using imagers to record absorption variations caused by microvascular blood volume pulsations, shows promise as a non-contact cardiovascular sensing technology. The first long-range imaging photoplethysmography measurements at distances of 25, 50, and 100 meters from the participant was recently demonstrated. Degraded signal quality was observed with increasing imager-to-subject distances. The degradation in signal quality was hypothesized to be largely attributable to inadequate light return to the image sensor with increasing lens focal length. To test this hypothesis, a follow-up evaluation with 27 participants was conducted outdoors with natural sunlight illumination resulting in ~5-33 times the illumination intensity. Video was recorded from cameras equipped with ultra-telephoto lenses and positioned at distances of 25, 50, 100, and 150 meters. The brighter illumination allowed high-definition video recordings at increased frame rates of 60fps, shorter exposure times, and lower ISO settings, leading to higher quality image formation than the previous indoor evaluation. Results were compared to simultaneous reference measurements from electrocardiography. Compared to the previous indoor study, we observed lower overall error in pulse rate measurement with the same pattern of degradation in signal quality with respect to increasing distance. This effect was corroborated by the signal-to-noise ratio of the blood volume pulse signal which also showed decreasing quality with respect to increasing distance. Finally, a popular chrominance-based method was compared to a blind source separation approach; while comparable in measurement of signal-to-noise ratio, we observed higher overall error in pulse rate measurement using the chrominance method in this data.

Keywords: imaging photoplethysmography, pulse rate, imager, outdoor, sunlight, long-range imaging, independent component analysis (ICA), chrominance

1. INTRODUCTION

Non-invasive, non-contact, cardiovascular sensing using imaging photoplethysmography (iPPG) is now a widely-studied method. Similar to traditional photoplethysmography[1], iPPG is able to measure cardiac-synchronous changes in light absorption related to cyclic, volumetric changes in blood volume of the microvasculature of exposed skin. The greatest number of investigations to-date have been focused on the estimation of pulse rate (PR) from the blood volume pulse (BVP) signal extracted from recorded video. Additional attention has been paid to cardiovascular measures including pulse rate variability[2], respiration[3], and peripheral oxygen saturation[4]. Additionally, the enabling approaches to iPPG measurement have been evaluated in real-world clinical environments[5-8].

In order to improve the accuracy of iPPG such that it might be adopted outside of research, investigators have explored several different methods for recovering the best quality blood volume pulse from the collected video. Two promising methods include blind source separation, such as independent component analysis (ICA)[9], and chrominance-based methods. Both methods attempt to reach a better representation of the BVP from the raw red, green, and blue color channels originally measured from the video. Subsequent advancements on these methods have also been explored, including the use of multiple, synchronous imagers as inputs to ICA[10, 11] and developing finer tunings of the color space transformation to compose the BVP signal[12,13]. The progress, state-of-the-art, and outstanding challenges for iPPG are documented in several recent review articles on iPPG[14-19].

*[a] Ethan.Blackford.ctr@us.af.mil; *[b] Justin.Estepp@us.af.mil

Optical Diagnostics and Sensing XVII: Toward Point-of-Care Diagnostics, edited by Gerard L. Coté, Proc. of SPIE Vol. 10072, 100720S · © 2017 SPIE · CCC code: 1605-7422/17/$18 · doi: 10.1117/12.2253460

Since the primary benefit of iPPG sensing is that measurements can be performed without requiring physical contact and at some distance away from the patient or participant, it is logical to test the impact of distance on BVP waveform quality and, ultimately, accuracy of physiological features of interest, as compared to ground-truth measures. A recent survey of distances used in iPPG studies revealed a range of 0.05 to 3 meters[20]. Recent work has sought to extend the upper range over which iPPG measurements had been made to distances up to 100 meters[20, 21] from the participant. In this work, a general trend of deteriorating data quality with increasing distances was observed[20]. Further, beyond 25 meters, the quality and consistency of the blood volume pulse signal had deteriorated to the point where individual BVP waves could no longer be accurately detected for measurements of instantaneous pulse rate, or pulse rate variability[21]. This effect was hypothesized to largely be the result of diminishing light return to the image sensor with increasing lens focal lengths which were to compensate for increased imager-to-participant distances. The change in light transmitted through a lens at different focal lengths is inversely proportional to squared ratio of the focal lengths. In previous evaluations, artificial, controlled lighting was used, thus limiting the total intensity of illumination that could be provided. As a result, the image sensor did not receive adequate amounts of light at longer focal lengths. That is, four times less light was transmitted to the image sensor for the greatest focal length, 1300 mm (required for the longest distance, 100m), as compared to the focal length used at the 25m distance, 650mm.

To determine if these long-distance measurements could be improved upon, this long-range study was replicated outdoors where natural sunlight was used as the illumination source. Hypothesizing that these new results may be an improvement over those previously shown, a distance of 150 meters was added to the previously-tested distances of 25, 50, and 100 meters. In a series of five-minute trials, video was recorded of stationary, seated participants while ground-truth electrocardiography (ECG) data were also recorded. Average pule rate for one-minute windows, as determined by the BVP signal extracted from the long-distance imager, was compared to the matching segments of heart rate (HR) from ground-truth ECG. These pulse rate measurements were subsequently used for correlation, Bland-Altman, and distribution analyses of the effect of distance. Additionally, an estimate of signal-to-noise ratio (SNR) of the extracted BVP signal waveform was also investigated. Finally, a chrominance-based method[22] for extracting the BVP waveform from the color data was compared to a blind source separation approach using the RGB color space[9, 20].

2. MATERIALS AND METHODS

2.1 Participants

27 participants (15 female, mean age of 23.6 years, age range of 19-47 years) were recruited for voluntary participation in this study. Of these 27 participants, 4 were wearing glasses, 11 maintained some form of facial hair, ranging from unshaven stubble to full beard, and 13 self-reported wearing at least one type of makeup or lotion on their face or neck. Since the data collection was performed outdoors in an exposed environment, all participants were offered SPF 50 sunscreen lotion to apply at the beginning of their session. In total, 8 of the participants applied sunscreen lotion to their face and/or neck (19 total with makeup, lotion, and/or sunscreen). All participants completed comprehensive informed consent prior to participation. This study was approved by the 711th Human Performance Wing Institutional Review Board and found to be in compliance with all relevant institutional and national/international guidelines for human subjects research. Participants were compensated for their time unless otherwise employed by the Department of Defense and in duty status at the time of their participation.

2.2 Data collection environment

Data collection took place in a large, open field in the Midwestern United States during the first three full weeks of July during daylight hours, and did not include any twilight or nighttime hours. A straight line-of-sight was formed between the participant, sitting at one end of the field, and the locations used for the video cameras placed at distances of 25, 50, 100, and 150 meters away from the subject for the various trials. The entire data collection lasted approximately 90 minutes. Natural sunlight provided the only form of illumination during video recording. In between the five-minute trials, participants were allowed to shelter in the shade to avoid over-exposure to the sun (sunburn, dehydration, etc.). During the trials themselves, they were seated in the open, without covering of shadow or shade, to ensure maximum illumination. A solid-gray partition was placed behind the participant to provide a consistent and neutral background and to eliminate the introduction of background image noise. Data collection was only suspended during periods of precipitation or high wind. Data collection for any single participant did not require interruption due to adverse experimental conditions. The data collection environment is shown in Figure 1.

Figure 1. An example of the physical configuration for data collection. The physiological signal acquisition unit is located to the right of the participant

2.3 Imaging equipment

The imagers used in this experiment were mirrorless digital cameras (Panasonic Lumix DMC-GH4, Panasonic, Kadoma, Osaka, Japan) equipped with fully-manual, super-telephoto lenses (650Z-B, Rokinon, New York, NY, United States) with a focal length range of 650-1300 mm and corresponding f-numbers of *f*/8-16. The f-number was determined solely by the focal length of the lens, as the lens does not contain an aperture element. For the longest distance of 150 m, an additional lens element, a 2x teleconverter (Rokinon, New York, NY, United States), was used to double the maximum effective focal length of the lens to 2600 mm. The imagers themselves were mounted to tripods and adjusted in height to be approximately even in height with a seated participant's face. The aim of the imager was adjusted so that the image was level with the horizon, the participant was centered in the image horizontally, and the participant's entire head and as much of the upper torso as possible was present in the image frame. The frame shutter/exposure speed was the adjusted to ensure a suitable frame exposure. Prior to each trial, the camera's internal light metering (multiple mode) was used to manually adjust the frame exposure to an ideal level. This was visualized as a non-saturated and center weighted image luminance histogram on the camera interface. Video was recorded in 1920x1080 FHD resolution. A native, intra-frame, H.264-based, compression algorithm with a maximum bit rate of 200 Mbps was used. Videos were recorded in the .MP4 format to an internal SD card (64GB Extreme PRO SDXC UHS-II, SanDisk, Milpitas, California, United States). To compensate for the additional lens element required to achieve an adequate zoom for the 150 m trial and the corresponding decrease in light transmittance, an increased ISO sensitivity, decreased frame rate, and increased allowable exposure speed were used for this trial in order to provide adequate image exposures. The specific lens and camera settings for each distance are provided in Table 1.

Table 1. Lens and Camera Settings by Distance.

Distance (m)	Focal Length (mm)	*f*/	Shutter Speed (s)	ISO	White Balance (K)	Resolution (px)	Frame Rate (fps)
25	650	8	≤1/60	200	6000	1920x1080	59.94p
50	~800	~9.5	≤1/60	200	6000	1920x1080	59.94p
100	1300	16	≤1/60	200	6000	1920x1080	59.94p
150	2600	32	≤1/30	400	6000	1920x1080	29.97p

2.4 Sunlight illumination

Natural sunlight provided the illumination source for all participants in this study; no additional artificial or controlled lighting was used. Illumination conditions were measured, at the location of the participant's face, prior to the start of each five-minute trial. Over all participants in the study, the range of lighting exposure conditions were measured to be 4,800-33,333 lx using a Litemaster Pro L-478DR exposure meter (Sekonic, North White Plains, New York, United States). There was no minimum or maximum illumination intensity threshold set as a requirement for data collection. Light intensity was measured at the beginning of each five-minute trial. There was considerable variability in illumination levels, even within individual trials due to changing cloud cover. Furthermore, over the course of the entire data collection there were significant changes in sunlight intensity related to cloud cover and time of day. Illuminance measurements are shown in Figure 2.

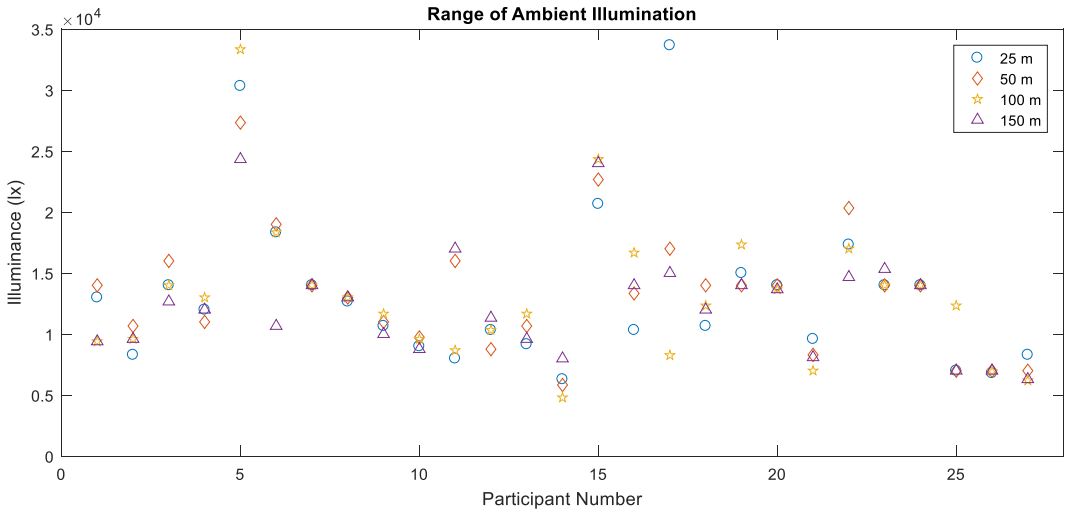

Figure 2. Ambient illumination as measured at the beginning of each five-minute trial. Illuminance was measured at the position of the subject's face and is not expected to vary based on the trial distance; however, distance is noted to show there was not an observable relationship between the distance trial order and illumination level.

2.5 Ground-truth physiology

Electrophysiological signals were acquired from each participant with a BioSemi ActiveTwo biopotential amplifier and data acquisition system (BioSemi B.V., Amsterdam, The Netherlands). Data were recorded to a workstation-class laptop at a digitization rate of 16,384 Hertz in BDF format using BioSemi's open-source data acquisition software, ActiView. ECG was recorded from a bipolar pair of active electrodes placed on the manubrium of the sternum, superior to the manubriosternal joint, and the left clavicle. The CMS and DRL electrodes of the BioSemi system were both placed on the right clavicle, separated by ~3 centimeters. Additional physiological signals, including galvanic skin response, respiratory effort, and fingertip, reflectance photoplethysmography were also collected during this study but are not components of this analysis.

2.6 Experimental design

Prior to the beginning of the study, a random trial order was determined. Each trial corresponded with a distance from the participant at which the imager was placed, resulting in a within-subjects design for the imager-to-participant distance factor. The order of distances 25, 50, and 100 m were randomized and performed first. The distance of 150m necessitated an additional lens element and different camera settings from the other three trials and was always performed last. Trials were then completed in the predetermined order. Trials that were incomplete due to error, interruption, or hardware failure (e.g. battery failure) were repeated in sequence. During data collection, participants were asked to sit quietly, in a relaxed position, and maintain a forward-facing direction for the entirety of the trial. Since sunglasses were not permitted, as they would have obscured a part of the face, participants were permitted to sit with their eyes closed during data collection to improve their comfort.

2.7 Analysis of ground-truth physiological data

The goal of this analysis was to compare average pulse rate over one-minute windows as obtained from the video data sources to the ground truth physiology as measured with ECG, for each imager-to-subject distance. To derive pulse rate estimates from the ECG, custom-written software written in MATLAB 2011b (The Mathworks, Inc., Natick Massachusetts, United States) was used to select R-R intervals in the filtered time series. An automated R-wave detection algorithm[23, 24], combined with subject-matter expert review and correction, provided the final set of R-R intervals for each trial. These R-R intervals, or inter-beat intervals (IBIs), were calculated for each pair of cardiac cycles in the recorded time series. The IBI time series were then windowed and averaged into five, one-minute, non-overlapping windows. The ground-truth measurement of heart rate (HR), in beats per minute (bpm), was then calculated from the one-minute windows.

2.8 Analysis of video data

Custom MATLAB code was developed to process the video data and analyze the extracted BVP waveform. A static ROI, centered on the participant including their head to upper shoulders was determined for each recording. Example frame regions extracted from the recorded videos and analyzed to extract the BVP waveforms are shown in Figure 3.

Figure 3. From top to bottom, images were captured at 25, 50, 100, and 150 meters. (Left) Cropped image regions, used for BVP extraction. (Center) Original video frames captured with the focal lengths specified in Table 1. (Right) Images captured with a standard lens (focal length of 14mm), to show scale. Decreased visual image quality is noted at greater distances and corresponding longer focal lengths. At longer focal lengths, the lens cannot focus as well compared to shorter focal lengths. Ground heat distortion was also observed in the images. As expected, this distortion increased with distance.

The selected region was decomposed into constituent red, green, and blue pixel spaces from which average color intensities were calculated for each frame, thus creating the RGB time series for each camera (one red, green, and blue time series for each camera). One-minute windows corresponding to the same time periods used in the ECG heart rate calculation were then selected and segmented. Each one-minute RGB time series was normalized to zero-mean, unit-variance and bandpass filtered from 0.3-11 Hz using a zero-phase, elliptical bandpass filter implementation.

To recover the BVP waveform from the RGB time series, a blind source separation approach utilizing independent component analysis was applied to decompose the RGB time series into source-space components. The extended infomax algorithm[25] as implemented in EEGLAB[26] was used to perform the ICA decomposition. Following ICA, the resulting components were bandpass filtered from 0.3-6 Hz using a zero-phase, elliptical bandpass filter implementation and upsampled to 1200 Hz using cubic spline interpolation.

Recovery of the BVP component from source space was achieved by identifying the component containing the largest ratio of peak power in a range of anticipated pulse rate frequencies compared to the power contained within all of the other frequencies in that anticipated range. To do so, the periodogram method, using a Hamming window, was applied to each component for spectral power density estimation. The peak power density within the range of [0.8, 2] Hz was the identified. Power in a band ± 0.2 Hz from the peak power frequency was calculated and compared to power calculated over all other frequencies in the [0.8, 2] Hz range, mutually exclusive of the frequencies contained within the peak power band. The independent component with the highest ratio of peak power to the remaining power in the band was selected as the BVP waveform component. The frequency at which the peak power was centered, f_{max}, was then converted to beats per minute (i.e., 60 *f_{max}). This method is analogous to that which has been applied previously[20, 21] as an adapted ICA-based approach[9]. Sample, BVP component time series, recovered using the ICA method, are shown in Figure 4.

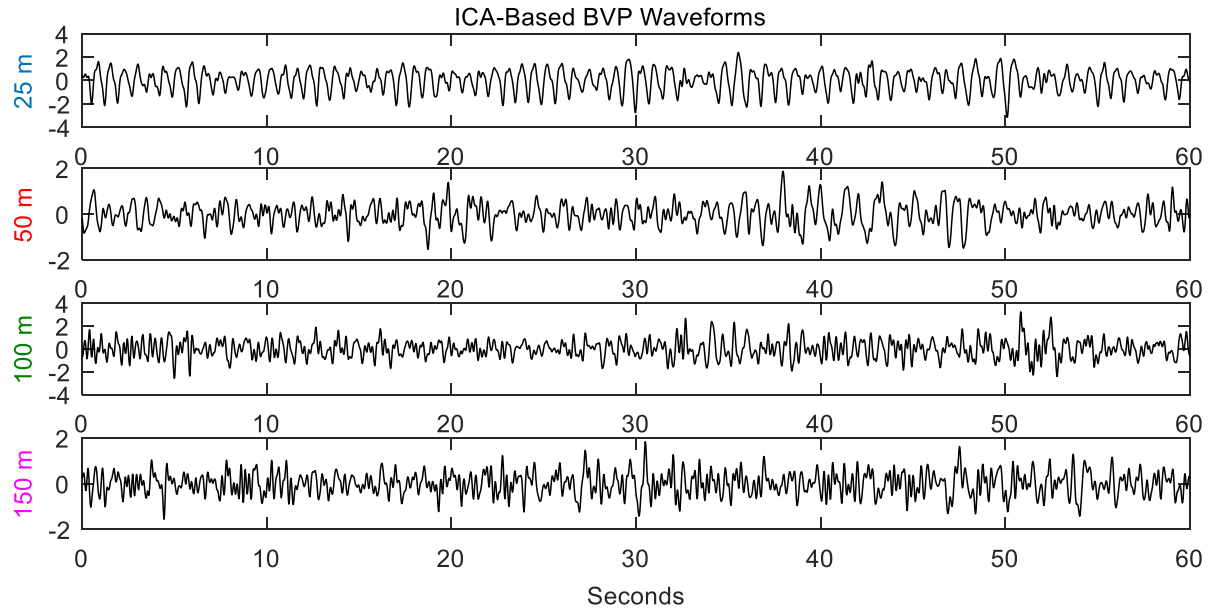

Figure 4. Characteristic blood volume pulse time series recovered with the ICA-based method. The first, one-minute windows are shown for each distance trial, for participant 20. From top to bottom, the signals were captured at imager-to-subject distances of 25, 50, 100, and 150 meters. Individual BVP waves are easily distinguished in the 25 m time series. Diminished signal quality is noted with increased distance.

Alternatively, a chrominance-based approach[22] was also applied to recover the BVP waveform. This method extracts the BVP using a difference of filtered and normalized chrominance components and inherently eliminates specular reflections which might otherwise create signal noise. The BVP is more ideally represented in the chrominance versus the RGB color space, where the channels are significantly correlated. The chrominance method assumes white illumination and a uniform skin-tone vector for all subjects. This vector was evaluated as suitable for a large range of different skin tones[22]. If these assumptions are acceptable, the method can be uniformly applied. This simplicity is an inherent strength of the method. However, subsequent methods do not require these assumptions[13].

To implement this method, two chrominance components, X_S and Y_S, are calculated from the normalized R, G, and B time series as follows:

$$X_s = 3R_n - 2G_n \qquad Y_s = 1.5R_n + G_n - 1.5B_n$$

The chrominance components X_S and Y_S are then filtered with an elliptical, bandpass filter between [0.75, 4] Hz to become X_f and Y_f. The chrominance signal, S, is then calculated as:

$$S = X_f - \alpha Y_f \quad \text{where} \quad \alpha = \sigma(X_f)/\sigma(Y_f) \quad \text{and} \quad \sigma(X_f) \text{ represents the standard deviation of } X_f$$

This method was then applied as an alternative method to extract the BVP. Sample chrominance signals are shown in Figure 5.

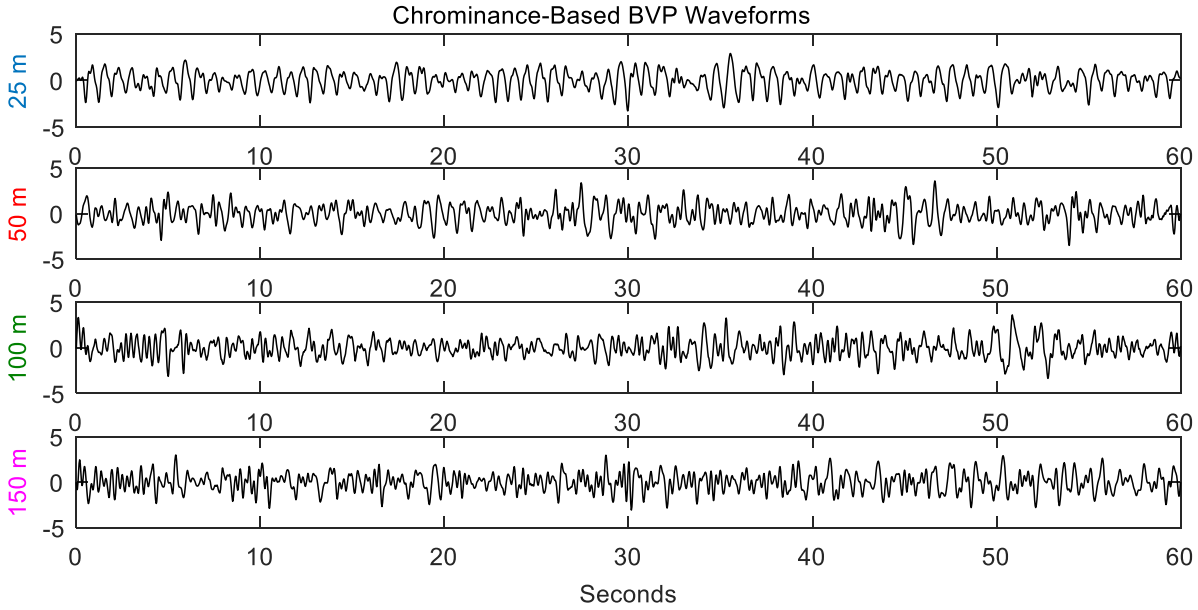

Figure 5. Characteristic blood volume pulse time series recovered with the chrominance-based method. The first, one-minute windows are shown for each distance trial, for participant 20. From top to bottom, the signals were captured at imager-to-subject distances of 25, 50, 100, and 150 meters. Similar to the ICA-based BVP extractions in Figure 4, individual BVP waves are easily distinguished in the 25 m time series. Diminished signal quality is again noted with increased distance.

2.9 Estimation of signal-to-noise ratio

The signal-to-noise ratio calculation for the BVP waveform was adapted from the method presented by de Haan and Jeanne[22]. The method presented used a 512 point FFT of a given time sample and calculated ratios of powers contained in specific bins of the FFT. A generalized version, adapted from this method was used in this work. The calculation involved the following steps. A periodogram method, using a hamming window, was calculated for each time series subsequent to the signal processing described in the above sections. For each window, the spectral peak corresponding to the ECG heart rate frequency was identified. The power contained within a window of ±0.1 Hz surrounding the ground-truth HR frequency and ±0.2 Hz surrounding its first harmonic were summed together and divided by the sum of all frequencies outside of these regions but within the range of 0-4Hz. The SNR was then transformed to decibels by multiplying its common logarithm by a factor of 10.

2.10 Comparisons with respect to distance and BVP extraction method

The primary experimental factor in this study is the imager-to-participant distance, with factor levels of 25, 50, 100, and 150 meters. Mean absolute error (MAE) between the measured HR (from ECG) and estimated pulse rate (from the BVP waveform) is compared across the factor levels, alongside estimated BVP SNR. A secondary factor, waveform extraction method, was also investigated. Two different BVP waveform extraction techniques were tested. The first is an ICA-based method[9, 20]; the second is a chrominance-based method[22].

3. RESULTS

A comparison of MAE distributions for the ICA and chrominance extraction methods, for each of the imager-to-participant distances is shown in Figure 6. A bootstrapping procedure was used to randomly sample a single, one-minute window from each participant and estimate the group average of the MAE. This bootstrapping procedure was repeated 1000 times; the resulting distribution of the bootstrapped, group-average MAE is shown as a boxplot distribution.

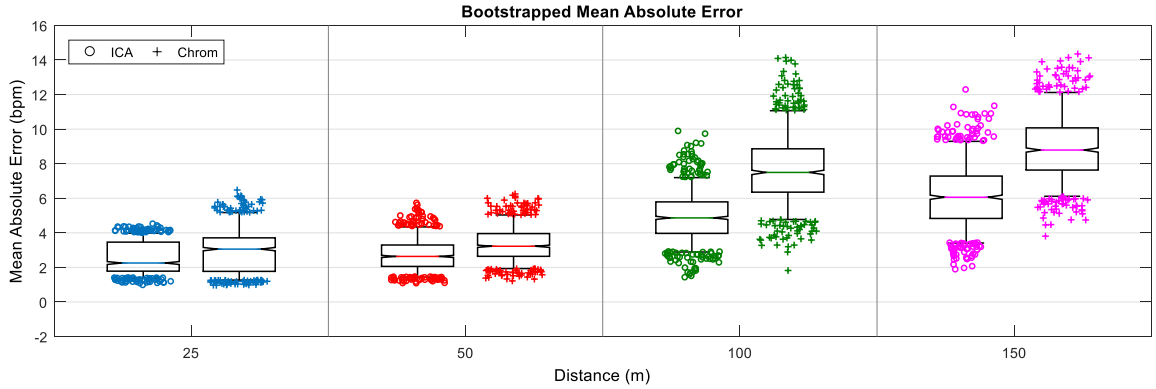

Figure 6. Box plots of bootstrapped mean absolute error, grouped by imager-to subject distance. Results from ICA-based and chrominance-based BVP extraction methods are shown. Whiskers depict the 95% CI of the bootstrapped distribution, with outlying points plotted individually. The notch is calculated as $1.58*IQR/\sqrt{\#\text{ Bootstrap Samples}}$.

An analysis of the SNR estimate is shown in Figure 7. Box plots are created from the average of the five, one-minute windowed estimates of BVP SNR, for each participant and distance level combination. SNR distributions are shown for each extraction method.

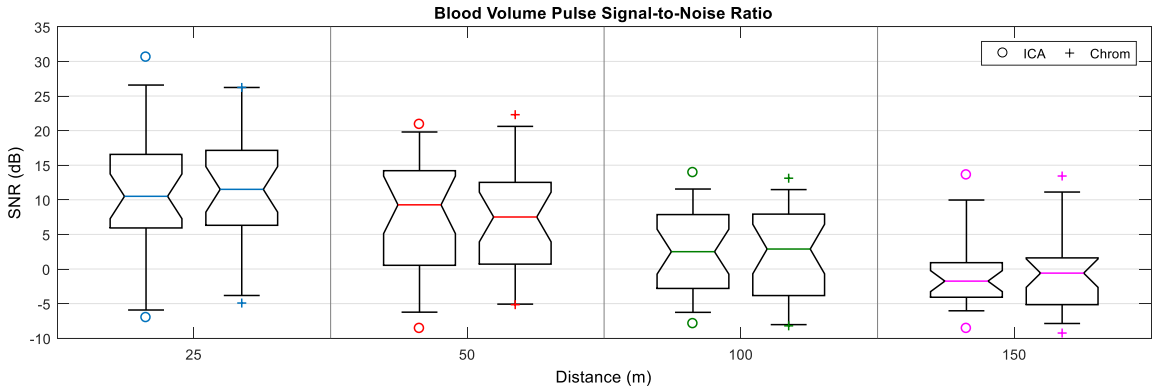

Figure 7. Box plots of signal-to-noise ratio, grouped by imager-to subject distance. Results from ICA-based and chrominance-based BVP extraction methods are shown. For each trial, the five, one-minute windows were averaged to create one point in the distribution. Whiskers depict the 95% CI of the distributions, with outlying points plotted individually.

Figures 8 shows the correlational and Bland-Altman[28, 29] analyses of MAE for both the ICA and chrominance extraction methods. In each case, the five, one-minute windows for each trial were averaged together such that each participant only contributed a single data point for each of the analyses (N = 27).

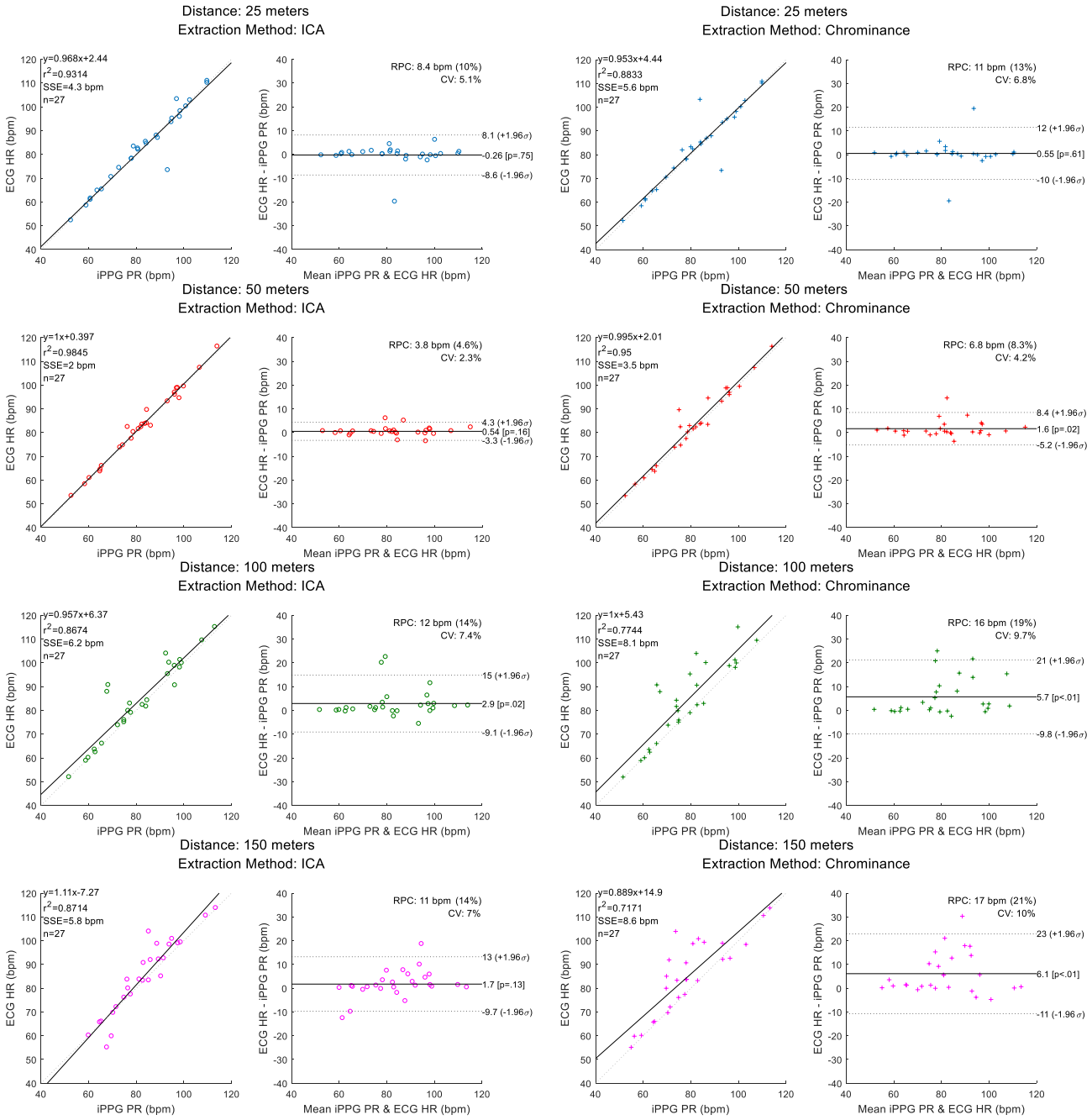

Figure 8. Correlation and Bland-Altman plots for iPPG PR compared to ECG HR. Each trial distance (by row) is shown for ICA (left) and chrominance (right) based BVP extraction methods. The correlation plots contain the linear regression equation, correlation coefficient (r^2), sum of squared error (SSE) and number of points. The Bland-Altman plots contain the reproducibility coefficient (RPC = 1.96*σ), and also show the coefficient of variation (CV = the standard deviation (σ) as a percentage of the mean), limits of agreement (LOA = ±1.96*σ), and the bias offset of the measures.

4. DISCUSSION

Given the inherent advantage presented by imaging photoplethysmography's ability to make measurements from a distance away from the patient or participant, it is worthwhile to investigate what range of distances and hardware configurations may be most suitable to obtain quality physiological data, and in particular, maintain desirable features in the extracted BVP morphology. When imaging at a distance, illumination is certain to be a critical factor, and ambient or environmental illumination may not be sufficient at certain ranges. To circumvent the challenges associated with providing adequate, controlled illumination, we replicated a previous study investigating imager-to-participant distance in an iPPG system. In this work, participants were measured outside in a natural, sunlight-illuminated environment. We tested the accuracy of pulse rate estimation, as determined by the extracted BVP waveform versus ECG-derived HR measurements for imager-to-participant distances of 25, 50, 100, and 150 meters. We also compared the extraction method used previously for long-range iPPG, ICA[20, 21], with a chrominance-based extraction method[22]. In addition to evaluating pulse rate estimation accuracy through MAE, we also used an estimate of signal-to-noise ratio in the extracted BVP waveform to further quantify the effects of both distance and extraction method on the BVP waveform that was derived from the recorded videos. Despite several challenges for measuring iPPG outdoors, the method showed overall improvements from those seen in a previous, indoor study. Some of these challenges included: variable lighting conditions, caused by changes in cloud cover, wind gusts disturbing the long range imager, which magnifies disturbances for the longest focal lengths, and quite pronounced atmospheric, heat distortions.

The correlation and Bland-Altman analyses, shown in Figure 8, show trends amongst the factors that tend to indicate higher error at longer distance and also larger errors in the chrominance-based method over the ICA-based method. Table 2 summarizes several key parameters from these results. It is possible that for this case with seated, stationary participants the ICA method was effective in determining a more optimal linear combination of source signals than achieved using the chrominance-based method, which is uniformly applied across all participants. This may not necessarily be the case in the presence of motion artifact, which was not a designed component of this study.

Table 2. Median, heart rate mean absolute error, and blood volume pulse signal-to-noise ratio, correlation (r^2), and Bland-Altman limits of agreement (LOA) results for analyses of the ICA and chrominance BVP extraction methods. Results are shown for each imager-to-subject distance.

	MAE (bpm)		**BVP SNR (dB)**		**Correlation: r^2**		**LOA: ±1.96σ (bpm)**	
Distance (m)	ICA	Chrom	ICA	Chrom	ICA	Chrom	ICA	Chrom
25	2.53	3.02	10.56	11.71	0.93	0.88	16.7	22.0
50	2.75	3.37	7.79	7.12	0.98	0.95	7.6	13.6
100	4.94	7.66	2.62	2.01	0.87	0.77	24.1	30.8
150	5.98	8.38	-0.91	-0.89	0.87	0.72	22.7	34.0

The trend of increasing MAE with increased imager-to-participant distance is also evident in Figure 6. This trend is similar to that found in previous long-range testing indoors with controlled, experimental lighting[20], though the median MAEs from the bootstrap procedure appear to be lower than those previously reported. A comparison of previous, indoor results and the outdoor results, presented in this work, for long-range iPPG is shown in Table 3.

Table 3. A comparison of mean absolute error in indoor and outdoor testing of long-range iPPG using ICA extraction of the BVP waveform. The trend of increased MAE with respect to distance is evident in both the indoor and outdoor data. However, the increased illumination provided by natural sunlight in the outdoor case, as compared to the artificial, controlled lighting in the indoor case, may have helped to reduce the MAE at comparable distances.

	Median MAE (bpm)	
Distance (m)	Indoor	Outdoor
25	2.0	2.3
50	4.1	2.6
100	10.9	4.9
150	-	6.1

The other trend that seems evident from Figure 6, but perhaps is not so obvious in Figure 8, is higher MAEs using the chrominance extraction method, as compared to the ICA extraction method. This trend is evident for all distances, although it also appears that there could be an interaction effect if a formal statistical analysis were to be performed (e.g., the increase in MAE in the chrominance method may increase with imager-to-participant distance, as well). Interestingly, the signal-to-noise ratio results shown in Figure 7 do not show evidence of any striking difference between the chrominance and ICA extraction methods, although there is a noticeable decline in SNR with respect to distance that is commensurate with the increase in MAE.

The totality of these results indicates that iPPG methods may be successfully applied at greater distances than have typically been investigated[20]. What may now be considered to be a predictable and repeatable effect of increased error and decreasing SNR with respect to distance was found; although the effect of increased illumination intensity in the outdoor setting may facilitate longer distances before becoming detrimental. Table 3 would indicate that at 50 meters, for the ICA extraction technique, the median MAE from the bootstrapping procedure remained less than 3 bpm for the data collected outdoors. By comparison for the previously-reported indoor data, median MAE was in excess of 4 bpm. While the median MAEs at 25 meters appear to be comparable (2.0 and 2.3 bpm for indoor and outdoor, respectively), the same trend observed at 50 meters is also evident at 100 meters (10.9 and 4.9 bpm for indoor and outdoor, respectively).

In a very preliminary investigation comparing the chrominance method to the ICA method for BVP waveform extraction, there would appear to be a difference in MAE, but not SNR. Yet, the SNR measure appears to be sensitive to increased imager-to-participant distances in a similar trend as MAE. In future work, researchers may consider including both physiological features, such as pulse rate, as well as an analysis of SNR. This may be useful because one measure may not always be predictive of the other. Future studies to develop an improved measure of BVP signal quality may also be beneficial.

5. CONCLUSIONS

In summary, a replication of previously-reported effects of long imager-to-subject distances for imaging photoplethysmography was performed. In this work, increased illumination levels provided by natural sunlight, as compared to previous, artificial lighting, appeared to be beneficial with respect to maintaining BVP waveform quality over long distances. Future attention should be paid to optimal BVP waveform extraction methods, such as chrominance versus blind source separation, or other methods yet to be developed. Each extraction methods may be preferable in certain situations over others. It may also be interesting to investigate hybrid methods, i.e. the use of the chrominance method in multi-imager studies such that it may be integrated with blind source separation approaches. Finally, while our implemented measure of SNR appears to be sensitive to the effect of distance, it was in disagreement with the observed difference between the extraction methods. It is worthwhile to consider cases where SNR estimation may aid in development and interpretation of iPPG data; as well as where alternative estimates of signal quality may be more reflective of the results obtained from the ultimate physiological, vital sign feature of interest.

ACKNOWLEDGMENTS

The authors would like to thank Margaret A. Bowers (Ball Aerospace), Samantha L. Klosterman (Ball Aerospace), Alyssa M. Piasecki (Oak Ridge Institute for Science and Education), Jeffrey C. Bolles (US Air Force Research Laboratory), and Megan C. Cleary (Oak Ridge Institute for Science and Education) for their assistance with data collection and preparation of the data for analysis. The authors would also like to extend their sincerest gratitude to the Greene County Parks & Trails Department (Xenia, Ohio, United States) for their assistance with providing access to the park grounds for data collection; without their cooperation and assistance, this work would not have been possible. With appreciation, we acknowledge that this work is supported by the Air Force Office of Scientific Research (AFOSR) under Air Force Research Laboratory Task# 14RH07COR, ‘Non-Contact Cardiovascular Sensing and Assessment’.

DISCLAIMER

The views expressed in this paper are those of the authors and do not reflect the official policy or position of the United States Air Force, the Department of Defense, of the United States Government. Reference herein to any specific commercial product, process, or service by trade name, trademark, manufacturer, or otherwise, does not necessarily constitute or imply its endorsement, recommendation, or favoring by the United States Government. The views and opinions of authors expressed herein do not necessarily reflect those of the United States Government and shall not be used for advertising or product endorsement purposes.

REFERENCES

[1] Allen, J., "Photoplethysmography and its application in clinical physiological measurement," Physiol.Meas. 28(3), 1-39 (2007).
[2] Sun, Y., Hu, S., Azorin-Peris, V., Kalawsky, R. and Greenwald, S., "Noncontact imaging photoplethysmography to effectively access pulse rate variability," J.Biomed.Opt. 18(6), 061205-061205 (2013).
[3] van Gastel, M., Stuijk, S. and de Haan, G. , "Robust respiration detection from remote photoplethysmography," Biomedical Optics Express 7(12), 4941-4957 (2016).
[4] van Gastel, M., Stuijk, S. and de Haan, G. , "New principle for measuring arterial blood oxygenation, enabling motion-robust remote monitoring," Scientific Reports 6 (2016).
[5] Mo, W., Mohan, R., Li, W., Zhang, X., Sellke, E. W., Fan, W., DiMaio, J. M. and Thatcher, J. E. , "The importance of illumination in a non-contact photoplethysmography imaging system for burn wound assessment," Proc.SPIE, Photonic Therapeutics and Diagnostics XI (2015).
[6] Villarroel, M., Davis, S., Watkinson, P., Guazzi, A., McCormick, K., Tarassenko, L., Jorge, J., Shenvi, A. and Green, G., "Continuous non-contact vital sign monitoring in neonatal intensive care unit," Healthcare Technology Letters 1(3), 87-91 (2014).
[7] Klaessens, J. H., van den Born, M., van der Veen, A., Sikkens-van de Kraats, J., van den Dungen, Frank A and Verdaasdonk, R. M., "Development of a baby friendly non-contact method for measuring vital signs: first results of clinical measurements in an open incubator at a neonatal intensive care unit," SPIE BiOS, 89351P-89351P-7 (2014).
[8] Aarts, L. A. M., Jeanne, V., Cleary, J. P., Lieber, C., Nelson, J. S., Bambang Oetomo, S. and Verkruysse, W. , "Non-contact heart rate monitoring utilizing camera photoplethysmography in the neonatal intensive care unit: A pilot study," Early Hum.Dev. 89(12), 943-948 (2013).
[9] Poh, M.-Z., McDuff, D. J. and Picard, R. W., "Advancements in Noncontact, Multiparameter Physiological Measurements Using a Webcam," Biomedical Engineering, IEEE Transactions on 58(1), 7-11 (2011).
[10] Estepp, J. R., Blackford, E. B. and Meier, C. M., "Recovering pulse rate during motion artifact with a multi-imager array for non-contact imaging photoplethysmography," Systems, Man and Cybernetics (SMC), 2014 IEEE International Conference on, 1462-1469 (2014).
[11] Blackford, E. B. and Estepp, J. R., "Effects of frame rate and image resolution on pulse rate measured using multiple camera imaging photoplethysmography," Proc.SPIE, Medical Imaging: Biomedical Applications in Molecular, Structural, and Functional Imaging, 94172D, 1-14 (2015).
[12] Wang, W., Stuijk, S. and De Haan, G., "A novel algorithm for remote photoplethysmography: spatial subspace rotation," IEEE Transactions on Biomedical Engineering 63(9), 1974-1984 (2016).
[13] de Haan, G. and, van Leest, A., "Improved motion robustness of remote-PPG by using the blood volume pulse signature," Physiol.Meas. 35(9), 1913 (2014).
[14] Sun, Y. and Thakor, N., "Photoplethysmography Revisited: From Contact to Noncontact, From Point to Imaging," IEEE Trans. Biomed. Eng. 63(3), 463-477 (2016).
[15] McDuff, D. J., Estepp, J. R., Piasecki, A. M. and Blackford, E. B., "A survey of remote optical photoplethysmographic imaging methods," 2015 37th Annual International Conference of the IEEE Engineering in Medicine and Biology Society (EMBC), 6398-6404 (2015).
[16] Kranjec, J., Beguš, S., Geršak, G. and Drnovšek, J., "Non-contact heart rate and heart rate variability measurements: A review," Biomedical Signal Processing and Control 13(0), 102-112 (2014).
[17] Teichmann, D., Bruser, C., Eilebrecht, B., Abbas, A., Blanik, N. and Leonhardt, S., "Non-contact monitoring techniques - Principles and applications," Engineering in Medicine and Biology Society (EMBC), 2012 Annual International Conference of the IEEE, 1302-1305 (2012).
[18] Liu, H., Yadong Wang and Lei Wang, "A review of non-contact, low-cost physiological information measurement based on photoplethysmographic imaging," Engineering in Medicine and Biology Society (EMBC), 2012 Annual International Conference of the IEEE, 2088-2091 (2012).
[19] Hu, S., Peris, V. A., Echiadis, A., Jia Zheng and Ping Shi, "Development of effective photoplethysmographic measurement techniques: From contact to non-contact and from point to imaging," Engineering in Medicine and Biology Society, 2009. EMBC 2009. Annual International Conference of the IEEE, 6550-6553 (2009).

[20] Blackford, E. B., Estepp, J. R., Piasecki, A. M., Bowers, M. A. and Klosterman, S. L. , "Long-range non-contact imaging photoplethysmography: cardiac pulse wave sensing at a distance," Proc.SPIE, Optical Diagnostics and Sensing XVI: Toward Point-of-Care Diagnostics (2016).
[21] Blackford, E. B., Piasecki, A. M. and Estepp, J. R., "Measuring pulse rate variability using long-range, non-contact imaging photoplethysmography," Engineering in Medicine and Biology Society (EMBC), 2016 IEEE 38th Annual International Conference of the, 3930-3936 (2016).
[22] de Haan, G. and Jeanne, V. , "Robust Pulse Rate From Chrominance-Based rPPG," Biomedical Engineering, IEEE Transactions on 60(10), 2878-2886 (2013).
[23] Pan, J. and Tompkins, W. J., "A Real-Time QRS Detection Algorithm," Biomedical Engineering, IEEE Transactions on BME-32(3), 230-236 (1985).
[24] Hamilton, P. S. and Tompkins, W. J., "Quantitative Investigation of QRS Detection Rules Using the MIT/BIH Arrhythmia Database," Biomedical Engineering, IEEE Transactions on BME-33(12), 1157-1165 (1986).
[25] Lee, T., Girolami, M. and Sejnowski, T. J., "Independent Component Analysis Using an Extended Infomax Algorithm for Mixed Sub-Gaussian and Super-Gaussian Sources," (1999).
[26] Delorme, A. and Makeig, S., "EEGLAB: an open source toolbox for analysis of single-trial EEG dynamics including independent component analysis," J.Neurosci.Methods 134(1), 9-21 (2004).
[27] Bland, J., M. and Altman, D., "Statistical Methods for Assessing Agreement Between Two Methods of Clinical Measurement," The Lancet 327(8476), 307-310 (1986).
[28] Klein, R., "Bland-Altman and Correlation Plot," Mathworks File Exchange (2014). http://www.mathworks.com/matlabcentral/fileexchange/45049-blandaltman-and-correlation-plot. [Accessed: 02- Feb- 2016].